European Journal of Nuclear Medicine and Molecular Imaging (2023) 50:1216–1227
https://doi.org/10.1007/s00259-022-06059-2

ORIGINAL ARTICLE

[^{68}Ga]Ga-Pentixafor PET/CT imaging for in vivo CXCR4 receptor mapping in different lung cancer histologic sub-types: correlation with quantitative receptors' density by immunochemistry techniques

Ankit Watts[1] · Baljinder Singh[1] · Harmandeep Singh[1] · Amanjit Bal[2] · Harneet Kaur[1] · Ninjit Dhanota[3] · Sunil K. Arora[3] · Bhagwant R. Mittal[1] · Digambar Behera[4]

Received: 10 August 2022 / Accepted: 22 November 2022 / Published online: 9 December 2022

Abstract

Purpose In vivo CXCR4 receptor quantification in different lung cancer (LC) sub-types using [^{68}Ga]Ga-Pentixafor PET/CT and to study correlation with quantitative CXCR4 receptors' tissue density by immunochemistry analyses.

Methods [^{68}Ga]Ga-Pentixafor PET/CT imaging was performed prospectively in 94 (77 M: 17F, mean age 60.1 ± 10.1 years) LC patients. CXCR4 receptors' expression on lung mass in all the patients was estimated by immunohistochemistry (IHC) and fluorescence-activated cell sorting (FACS) analyses. SUV_{max} on PET, intensity score on IHC, and mean fluorescence index (MFI) on FACS analyses were measured.

Results A total of 75/94 (79.8%) cases had non-small cell lung cancer (NSCLC), 14 (14.9%) had small cell lung cancer (SCLC), and 5 (5.3%) had lung neuroendocrine neoplasm (NEN). All LC types showed increased CXCR4 expression on PET (SUV_{max}) and FACS (MFI). However, both these parameters (mean SUV_{max} = 10.3 ± 5.0; mean MFI = 349.0 ± 99.0) were significantly (p = 0.005) higher in SCLC as compared to those in NSCLC and lung NEN. The mean SUV_{max} in adenocarcinoma (n = 16) was 8.0 ± 1.9 which was significantly (p = 0.003) higher than in squamous cell carcinoma (n = 54; 6.2 ± 2.1) and in not-otherwise specified (NOS) sub-types (n = 5; 5.8 ± 1.5) of NSCLC. A significant correlation (r = 0.697; p = 001) was seen between SUV_{max} and MFI values in squamous cell NSCLC as well as in NSCLC adenocarcinoma (r = 0.538, p = 0.031) which supports the specific in vivo uptake of [^{68}Ga]Ga-Pentixafor by CXCR4 receptors. However, this correlation was not significant in SCLC (r = 0.435, p = 0.121) and NEN (r = 0.747, p = 0.147) which may be due to the small sample size. [^{68}Ga]Ga-Pentixafor PET/CT provided good sensitivity (85.7%) and specificity (78.1%) for differentiating SCLC from NSCLC (ROC cutoff SUV_{max} = 7.2). This technique presented similar sensitivity (87.5%) and specificity (71.4%) (ROC cutoff SUV_{max} = 6.7) for differentiating adenocarcinoma and squamous cell variants of NSCLC.

Conclusion The high sensitivity and specificity of [^{68}Ga]Ga-Pentixafor PET/CT for in vivo targeting of CXCR4 receptors in lung cancer can thus be used effectively for the response assessment and development of CXCR4-based radioligand therapies in LC.

Keywords [^{68}Ga]Ga-Pentixafor PET/CT · Lung cancer · CXCR4 receptors

This article is part of the Topical Collection on Oncology - Chest

✉ Baljinder Singh
drbsingh5144@yahoo.com

[1] Department of Nuclear Medicine, Postgraduate Institute of Medical Education & Research (PGIMER), Chandigarh 160012, India

[2] Department of Histopathology, Postgraduate Institute of Medical Education & Research (PGIMER), Chandigarh 160012, India

[3] Department of Immunopathology, Postgraduate Institute of Medical Education & Research (PGIMER), Chandigarh 160012, India

[4] Department of Pulmonary Medicine, Postgraduate Institute of Medical Education & Research (PGIMER), Chandigarh 160012, India

Introduction

18-Fluorine fluorodeoxyglucose-positron emission tomography [^{18}F]F-FDG-PET integrated with computed tomography (CT) as hybrid PET/CT imaging remains the mainstay for staging and diagnostic work-up in lung cancer (LC) patients [1, 2]. Nevertheless, [^{18}F] F-FDG-PET has limitations such as the inability to differentiate inflammatory/infectious pathologies from tumor/recurrence and has limited clinical utility for detecting brain metastasis due to high physiological tracer uptake in the normal brain cortex [3, 4]. It has been reported that there is no definite trend of [^{18}F] F-FDG-derived SUV_{max} values for differentiating small cell lung cancer (SCLC) from non-small cell lung cancer (NSCLC) [5]. In a recent study, it has been shown that FDG-derived SUV_{max} values are insufficient to predict prognosis in SCLC, though the whole-body metabolic tumor volume (MTV) reflecting total tumor load is a prognostic index in SCLC [6]. However, the SUV_{max} values have been reported to predict histological grade and pathological sub-type in lung adenocarcinoma [7]. In view of these drawbacks of [^{18}F] F-FDG-PET/CT imaging, development of newer PET radiopharmaceuticals with high specificity is highly anticipated [8].

Advances in molecular cancer biology have demonstrated that many of these promising tumor targets are receptors and have been reported as earliest targets for cancer diagnosis as well as precision therapy, with notable success in the effective treatment in few cancers [9]. An important class of targets is CXCR4—a chemokine receptor that is widely expressed in 30 different human cancers including lung carcinoma [10–12]. Recently, a CXCR4 targeting [^{68}Ga]Ga-Pentixafor PET tracer has gained attention in PET oncology [13–15]. This PET probe has exhibited promising results in a "first proof of concept" study in various solid tumors including lung carcinoma [16]. We have previously reported that [^{68}Ga]Ga-Pentixafor PET/CT picked up brain metastatic lesions quite distinctly in a patient with documented NSCLC which is a limitation of [^{18}F] F-FDG-PET [17]. In another study, we reported that [^{68}Ga]Ga-Pentixafor PET/CT offers high contrast images for the in vivo detection of CXCR4 expression in recurrent glioma [18]. In the present study, [^{68}Ga]Ga-Pentixafor PET imaging was performed to image the CXCR4 overexpression in various lung cancer sub-types and findings were validated with simultaneous tissue characterization and quantification of CXCR4 receptors by histopathological, IHC, and FACS analyses.

Materials and methods

This study was approved by the Institute ethic committee (IEC) as a PhD thesis protocol of the first author (AW). A written informed consent was obtained from all the patients enrolled in this study.

Patients

A total of 94 patients with biopsy-proven lung carcinoma were enrolled prospectively from July 2016 to March 2019. All the patients were subjected to either bronchoscopic or image-guided biopsy from the lung lesions. The tissue diagnosis was made on the basis of routine histopathological analysis of fixed lung tissue cores.

CXCR4 receptors' expression analysis

Immunohistochemistry (IHC) assay

Immunohistochemistry analysis was done on paraffin-embedded tumor sections to assess CXCR4 expression. The dewaxed slides after rehydration were incubated with the primary anti-CXCR4 monoclonal antibody UMB2 (AB124824, Abcam, Waltham, MA, USA) at room temperature in moist chamber for 1.5 h. After PBS wash, it was incubated with secondary antibody (Ab209101, Abcam, Waltham, MA, USA) conjugated with signal amplifier, horseradish peroxidase (HPR), for 45 min. Finally, dehydrated slides were used for visual scoring based on intensity of CXCR4-stained cells (1 +, 2 +, or 3 +) and percentage of CXCR4-positive tumor cells (5–10% = 1, 10–50% = 2, > 50% = 3) in the whole population of cells as seen under the microscope by an experienced pathologist. Final scoring was computed by considering both the criteria and the maximum score that could be attained was 9.0. The IHC analysis could be performed only in 60/94 (64.0%) of the study subjects. This included 31/54 (NSCLC squamous cell), 11/16 (NSCLC adenocarcinoma), 5/5 (NSCLC-NOS), 8/14 (SCLC), and 2/5 (lung NEN) respectively.

Fluorescence-activated cell sorting (FACS) analysis

Fresh lung tissue biopsy samples obtained in normal saline (NS) were processed to make single cell suspension. The cell suspension was divided equally into two falcon round bottom tubes. To label the CXCR4 cells in the single cell suspension, 5.0µL of phycoerythrin (PE)–labeled CD184 (BD PharMingen Inc., San Diego, USA) antibody was added to one of the tubes and the other tube was marked as unstained. The final stained and unstained tubes were subjected to FACS analysis (FACS-Calibur, BD PharMingen Inc., San Diego, USA). The data acquired for unstained cell population was used to set the gate for CXCR4-positive cell analysis. Mean fluorescence index (MFI) and percentage of stained CXCR4 cells were obtained as quantitative parameters.

[^{68}Ga]Ga-Pentixafor radiolabelling

The labeling of ^{68}Ga with Pentixafor was done under good manufacturing practice (GMP) condition in a fully automated synthesizer (Scintomics, Munich, Germany) procured under the DST-FIST grant (Government of India). The radiolabelling was done using the standard procedure as has been reported previously [19].

[^{68}Ga]Ga-Pentixafor PET/CT imaging

[^{68}Ga]Ga-Pentixafor PET/CT imaging was performed in all ($n=94$) patients at 60 min after intravenous administration of 111.0–185.0 MBq of the radiopharmaceutical. The whole-body PET/CT (using Discovery STE16/Discovery; 710/Discovery MIDR, GE Healthcare, Milwaukee, USA) acquisition was started at 1.0 h. Scanogram (120kVp and 10mAs) was done first to define the scan range for CT and PET whole-body scans. All the PET/CT machines were cross-calibrated periodically using different phantoms to ensure unified SUV output. Whole-body contrast-enhanced CT was done with the following acquisition parameters: voltage of 120 keV, current of 150–250mAs (smart modulated mA), slice thickness of 3.75 mm, tube rotation time of 0.5 s, pitch of 0.98:1, and matrix size 512 × 512. PET acquisition was done with 3 min/bed position for a total of 6 to 9 bed positions from the skull to proximal thighs in a caudocranial direction. Semi-quantitative analysis was done on reconstructed fused PET and CT images by computing SUV_{max} values of the primary lung tumor.

Statistical analysis

The statistical analysis was performed using the Statistical Package for Social Sciences (IBM, USA, SPSS statistics 20). Pearson's correlation analysis was applied between CXCR4 expression (MFI) and SUV_{max} values. A receiver operating characteristic (ROC) curve analysis was done to derive the cutoff values of SUV_{max}. All statistical tests were two-sided and were performed at a significance level of $p<0.05$.

Results

Ninety-four patients (77 M: 17F, mean age 60.1 ± 10.1 years; range 36–82 years) were recruited prospectively. Histopathological diagnosis confirmed that 75 patients had NSCLC with 54 as squamous cell variant, 16 as adenocarcinoma, and 5 as NOS, and 14 had SCLC and 5 had lung NEN (Table 1). A study from our center by Singh et al. reported the incidence of squamous cell carcinoma as 34.8%, followed by adenocarcinoma as 26.0% and small cell lung carcinoma as 18.4% [20]. Therefore, in the present study, the demographic profiling of lung cancer sub-types matched with this previous study from the same geographical region.

All sub-types of lung cancer showed increased tracer uptake in the primary lesions on [^{68}Ga]Ga-Pentixafor PET/CT which was indicative of high CXCR4 tumor positivity. Representative [^{68}Ga] Ga-Pentixafor MIP and axial-fused PET/CT images are presented comprehensively in Fig. 1 in one patient each of SCLC (A, B), NSCLC adenocarcinoma (C, D), NSCLC squamous (E, F), and lung NEN (G, H)

Table 1 Patients' details and the quantitative results of [^{68}Ga]Ga-Pentixafor PET/CT (SUV_{max}), FACS (MFI and percent stained cells), and IHC analysis in all study subjects

Histopathology	Sub-type (number of patients)	Sex (male:female)	Mean age (years)	[^{68}Ga]Ga-Pentixafor PET/CT imaging	Quantitative parameters of FACS analysis (mean ± SD)		Immunohistochemistry (IHC)
				SUV_{max} values (mean ± SD)	Mean fluorescence intensity (MFI) values	Percent stained cells (%)	Visual scoring (mean ± SD)
Non-small cell lung carcinoma (NSCLC)	Squamous cell ($n=54$)	49 M:5F	62.6 ± 9.5 (range = 39–82)	6.2 ± 2.1*	135.7 ± 80.1*	40.6 ± 21.4	5.1 ± 2.71 ($n=29$)
	Adenocarcinoma ($n=16$)	7 M:9F	56.6 ± 8.7 (range = 47–70)	8.0 ± 1.9 (n.s.)	288.3 ± 121.5 (n.s.)	47.7 ± 22.7	––
	NOS ($n=5$)	4 M:1F	61.2 ± 7.0 (range = 52–59)	5.8 ± 1.5*	159.8 ± 37.9*	39.4 ± 20.6	––
Small cell lung carcinoma (SCLC)	SCLC ($n=14$)	13 M:1F	62.5 ± 7.5 (range = 50–75)	10.3 ± 5.0	349.0 ± 98.5	45.6 ± 22.3	4.50 ± 4.0 ($n=8$)
Neuroendocrine neoplasm (NEN)	NET primary lung ($n=5$)	5 M:0F	50.0 ± 8.5 (range = 36–57)	5.2 ± 1.2*	60.6 ± 25.0*	26.0 ± 16.3	2 and 9 ($n=2$)

*$p<0.005$ w.r.t. to the SUV_{max} and MFI values of SCLC patients, n.s: not significant

respectively. The corresponding FACS histograms depicting the quantitative CXCR4 receptors' expression (MFI) and percent stained cells in these patients are presented in Fig. 2. Typically, the immunohistochemistry of stained sections of the lung mass using anti-CXCR4 antibody showing tumor positivity in patients of NSCLC squamous cell cancer is presented in Fig. 3A. Figure 3B demonstrates CXCR4-negative staining in a patient of NSCLC adenocarcinoma.

SCLC patients ($n=14$) showed a higher mean SUV_{max} value of 10.3 ± 5.0 (range 6.5–26.64; median = 8.9) as compared to all other types of lung cancer, and correspondingly a higher mean MFI value of 349.0 ± 98.5 was noted in SCLC. The percentage of CXCR4-stained cells was found to be $45.6 \pm 22.3\%$. IHC analysis could be performed in 8/14 patients. CXCR4 tumor positivity on the stained slides was observed only in 6/8 patients. The mean visual score was found to be 4.5 ± 4.0. No significant correlation was found in the SCLC group between SUV_{max} and MFI values ($r=0.435$, $p=0.121$), between SUV_{max} and percentage stained cells ($r=-0.036$, $p=0.902$), and between SUV_{max} and IHC visual score ($r=0.482$, $p=0.226$).

Among those in the NSCLC group, patients with adenocarcinoma ($n=16$) had a higher mean SUV_{max} value of 8.0 ± 1.9 (range 4.7–12.2; median = 7.7) and the corresponding mean MFI value of 288.3 ± 121.5, and the mean percentage of CXCR4-stained cells was $47.7 \pm 22.7\%$ respectively. A significant positive correlation ($r=0.538$, $p=0.031$) was found between SUV_{max} and MFI values. The graphs depicting the correlation between the SUV_{max} and MFI values in different histologic LC types are presented in Fig. 4. No significant correlation was found between SUV_{max} and the percentage stained cells ($r=0.129$, $p=0.634$). The IHC analysis was carried out in 11/16 patients with adenocarcinoma. However, none of the patients on IHC staining showed any evidence of a cytoplasmic CXCR4 tumor positivity despite that both FACS analysis and [^{68}Ga]Ga-Pentixafor findings suggested the presence of CXCR4 expression in all the patients.

In NSCLC squamous cell patients ($n=54$), the mean SUV_{max} value was estimated to be 6.2 ± 2.1 (range 3.2–15.0; median = 5.6) which was lower than the SCLC and adenocarcinoma patients. A similar trend was seen in the mean MFI values (135.7 ± 80.1) and the mean percentage of CXCR4-positive cells ($40.6 \pm 21.4\%$). The IHC analysis revealed CXCR4 tumor positivity on the stained slides in 29/31 patients and the mean visual scoring was estimated to be 5.1 ± 2.7. A highly significant ($r=0.690$, $p=0.0001$) positive correlation was observed between SUV_{max} and MFI values. Similarly, a significant correlation ($p<0.05$) was seen between SUV_{max} values and the percentage stained cells ($r=0.296$; $p=0.030$) in NSCLC (squamous cell only).

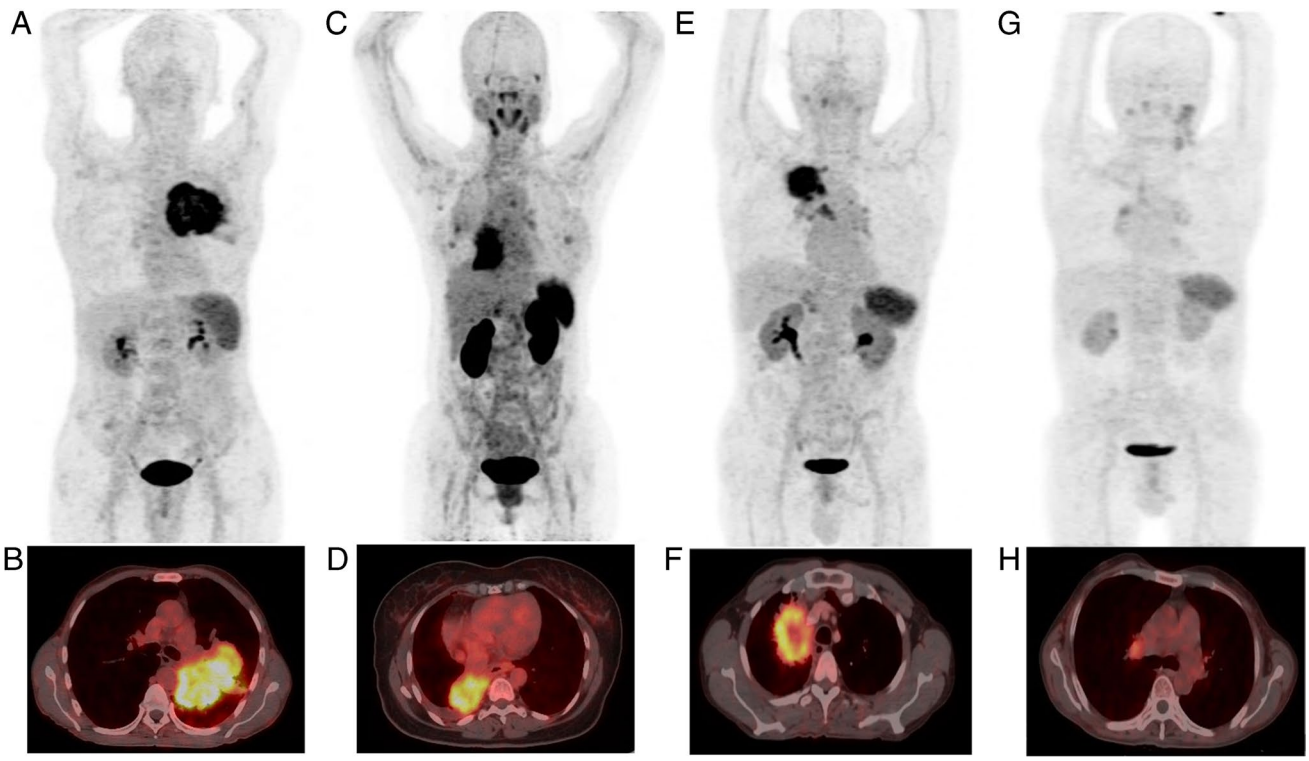

Fig. 1 [^{68}Ga]Ga-Pentixafor MIP and axial-fused PET/CT images in one patient each of SCLC (**A**, **B**) with $SUV_{max}=13.2$, NSCLC adenocarcinoma (**C**, **D**) with $SUV_{max}=12.2$, NSCLC squamous (**E**, **F**) with $SUV_{max}=7.2$, and lung NET (**G**, **H**) with $SUV_{max}=5.2$ respectively

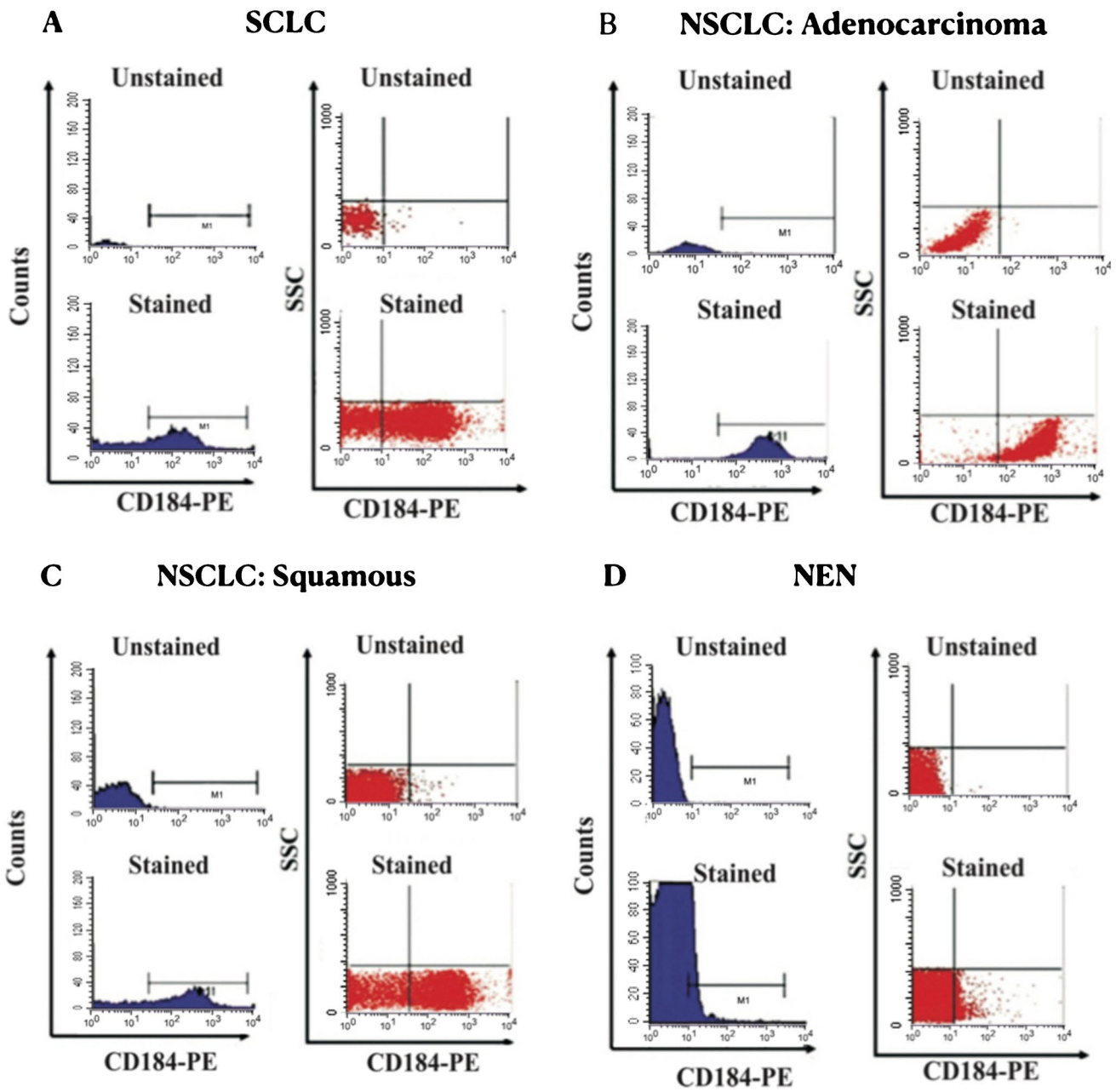

Fig. 2 Expressions of CXCR4 receptors using CD184 were quantified using flow cytometry. Quantification of receptor CXCR4 using CD184 was performed using both mean fluorescence intensity (MFI)-histograms and percentage positive population in dot plots. Gates were adjusted based on fluorescent negative unstained controls. Representative histograms and dot plots for CXCR4 and CD184 expression in patients' tumor specimen are presented in **A** for SCLC (MFI = 414.0), **B** for NSCLC:adenocarcinoma (MFI-289.0), **C** for NSCLC:squamous (MFI = 99.0), and **D** NEN (MFI = 100.0) respectively

No significant correlation between SUV_{max} and MFI was noted in any other group of patients.

In the NSCLC-NOS group ($n = 5$), the mean SUV_{max} value was found to be 5.8 ± 1.5 (median = 5.5). The corresponding mean MFI value was found to be 159.8 ± 37.9 and the mean percentage of stained CXCR4 expressing cells was estimated to be $39.4 \pm 20.6\%$. IHC analysis in this group did not reveal any histochemical evidence of the CXCR4 tumor positivity. No significant correlation between SUV_{max} and MFI values ($r = 0.851$, $p = 0.067$) and between SUV_{max} and the percent stained cells ($r = -0.037$; $p = 0.615$) was noted.

In NEN patients ($n = 5$), the mean SUV_{max} value was found to be 5.2 ± 1.2 (median = 5.1) and the mean MFI and the percentage stained cells were estimated to be 60.6 ± 25.0 and $26.0 \pm 16.3\%$ respectively. The IHC analysis

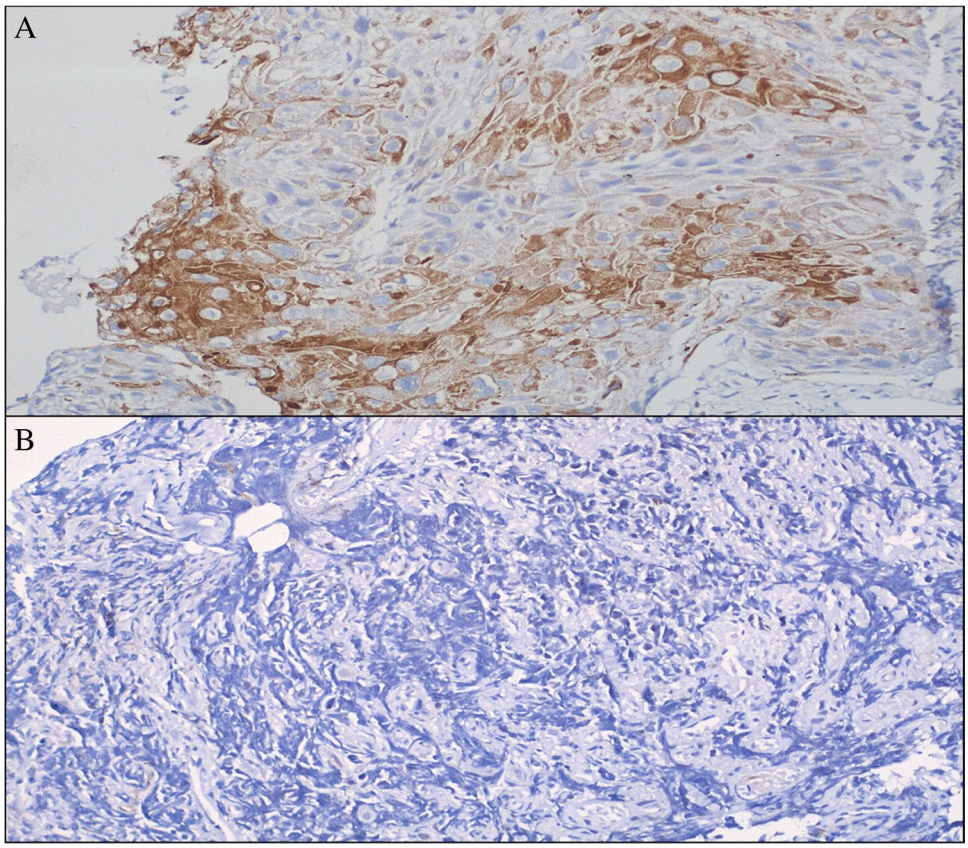

Fig. 3 Immunohistochemistry in paraffin-embedded lung tissue in a patient of NSCLC squamous cell carcinoma using anti-CXCR4 antibody showing 3 + CXCR4 intensity and > 50% stained tumor cells (**A**). The Fig **B** Demonstrates CXCR4 negative staining in a patient of NSCLC adenocarcinoma patient

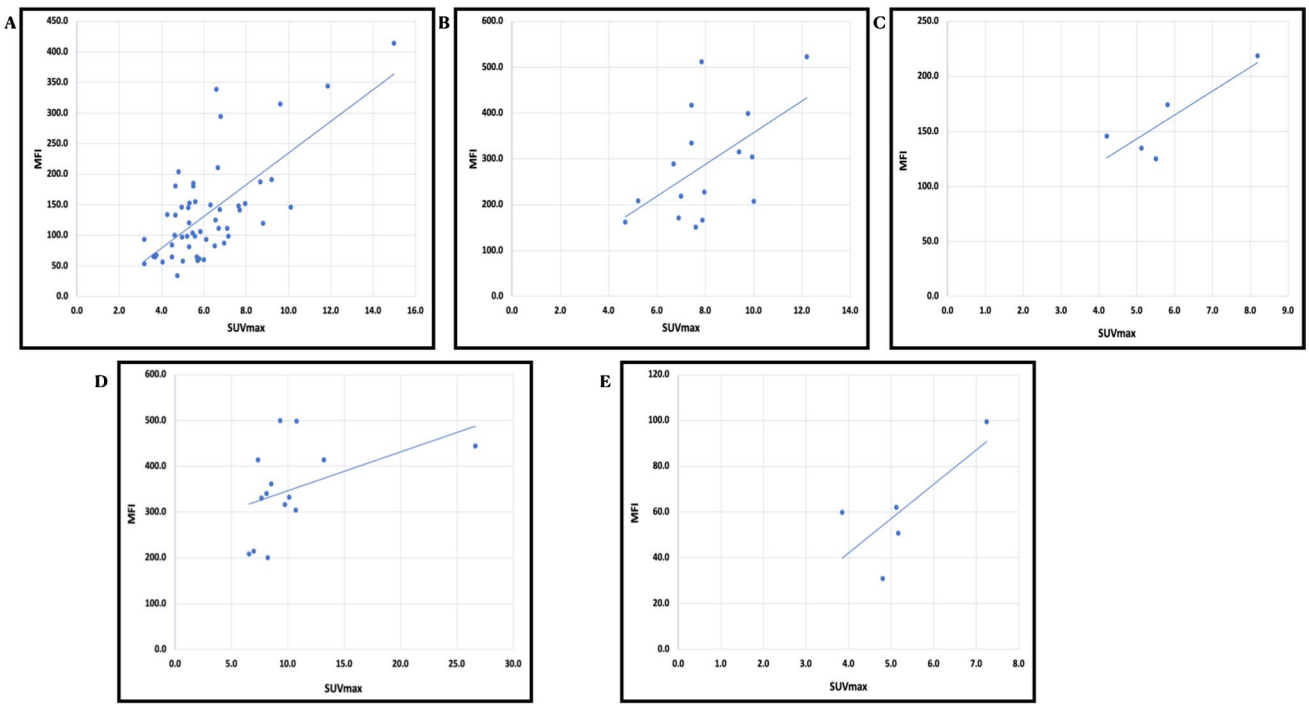

Fig. 4 A graphical representation for Pearson correlation (2-tailed significance) analysis between SUV_{max} and MFI in patients of NSCLC squamous cell (**A**), NSCLC adenocarcinoma (**B**), NSCLC-NOS (**C**), SCLC (**D**), and NEN (**E**) respectively

($n=5$) revealed that CXCR4 tumor positivity was observed only in 2/5 patients. There was no significant correlation between SUV_{max} and MFI values ($r=0.747$, $p=0.147$). Likewise, no correlation was seen between SUV_{max} and the percent stained cells ($r=-0.293$; $p=0.663$).

In the nutshell, [^{68}Ga]Ga-Pentixafor PET/CT findings showed increased tracer uptake (SUV_{max}) in the primary lung tumor in all the 94 (100.0%) patients. And the tracer uptake varied as a function of the quantitative CXCR4 receptors' density and both decreased in the order, viz., SCLC, NSCLC adenocarcinoma, NSCLC squamous, NOS, and lung NEN respectively. On the other hand, the IHC results were inconsistent and the CXCR4 tumor positivity rate was observed to be 62% (37/60) only and did not show any correlation with the SUV_{max} values in any of the LC sub-groups. In the present study, FACS analysis was done on the day of biopsy in fresh tissue sample, whereas the IHC was done retrospectively in paraffin-fixed stored samples and the inadequate sample for detailed IHC was the most common reason of not performing the CXCR4 staining in the remaining 34/94 patients. With the simultaneous use of two (FACS and PET-SUV_{max}) quantitative in vitro and in vivo techniques for documenting the CXCR4 expression, the absence or non-availability of IHC results in some patients have not affected the results of this study.

However, for the percentage stained cells, a positive correlation ($p=0.05$) was observed with SUV_{max} values only in the NSCLC squamous cell group of patients. The results of the correlation analysis among the various sub-types of the study subjects are presented in Table 2 and Fig. 4.

Table 2 Pearson correlation of SUV_{max} values with MFI and % stained cells in different lung cancer types

Parameters	Lung cancer sub-type				
	Squamous cell carcinoma ($n=54$)	Adenocarcinoma ($n=16$)	NOS ($n=5$)	SCLC ($n=14$)	NEN ($n=5$)
MFI	$r=0.690$; $p=0.0001$	$r=0.538$; $p=0.031$	$r=0.851$; $p=0.067$	$r=0.435$; $p=0.121$	$r=0.747$; $p=0.147$
% stained cells	$r=0.296$; $p=0.03$	$r=0.129$; $p=0.634$	$r=-0.307$; $p=0.615$	$r=-0.036$; $p=0.902$	$r=-0.293$; $p=0.633$

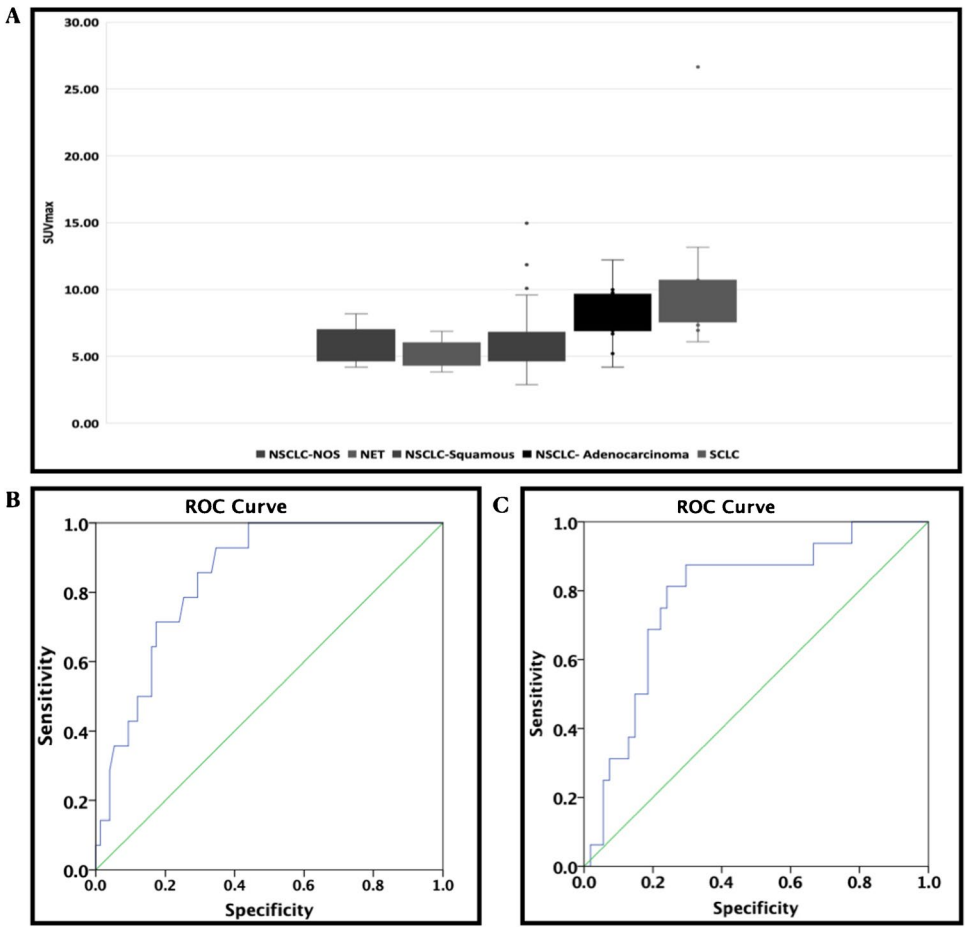

Fig. 5 The comparative Box and whisker plots showing differing SUV_{max} values in different histological types of NSCLC and SCLC (**A**). The ROC curve analysis (at SUV_{max} cutoff = 7.2) provided sensitivity (*x*-axis) and specificity (*y*-axis) of 85.7% and 78.1% for differentiating SCLC versus NSCLC (**B**). Similar ROC analysis provided sensitivity and specificity of 87.5% and 71.4% (at SUV_{max} cutoff = 6.7) for differentiating NSCLC adenocarcinoma and squamous cell variants (**C**)

Box and whisker plots analysis (Fig. 5A) demonstrated that the mean SUV_{max} value was significantly ($p = 0.005$) higher in the SCLC as compared to that in the NSCLC group (including all the variants). Similarly, the mean SUV_{max} value in SCLC was significantly higher than in the squamous cell lung cancer patients. However, the mean SUV_{max} value in adenocarcinoma patients did not differ significantly from that observed in SCLC patients.

The ROC curve analysis provided the SUV_{max} cutoff value for [^{68}Ga]Ga-Pentixafor uptake as 7.2. Using this value provided sensitivity and specificity of 87.5% and 72.0% respectively (Fig. 5B) for differentiating SCLC from NSCLC, while the estimated SUV_{max} cutoff value of 6.7 when used to differentiate adenocarcinoma from squamous cell carcinoma provided sensitivity and specificity of 87.5% and 71.4% respectively (Fig. 5C).

Discussion

The CXCR4/CXCL12 "receptor-ligand pair" plays a prominent role in cell proliferation and metastasis in at least 30 different human cancers [21, 22]. [^{68}Ga]Ga-Pentixafor—a CXCR4-targeting radioligand—allows in vivo visualization non-invasively of tumors expressing these receptors [13, 15]. The use of [^{68}Ga]Ga-Pentixafor PET/CT imaging has proven the potential of this tracer in evaluating the whole-body disease burden of CXCR4 receptors in many hematological and solid human malignancies [23]. Furthermore, high contrast PET images demonstrated by this tracer have led to the development of beta emitting ^{90}Y/^{177}Lu-Pentixather as a powerful ^{68}Ga and ^{90}Y/^{177}Lu theranostic pair [24–26]. This theranostic pair has been introduced successfully for the treatment of advanced-stage multiple myeloma, lymphoma, and leukemia [27–29].

CXCR4 stromal cell–derived 1-α factor is critical in cancer growth and metastasis. Typically, the rising activity of this factor in the lymph nodes, bone, bone marrow, lung, and liver has been reported to trigger the metastasis of CXCR4 expressing tumor cells [30, 31]. CXCR4 receptors' overexpression thus has been recognized as an adverse prognostic factor in various malignancies including lung cancer [32–34]. Therefore, [^{68}Ga]Ga-Pentixafor PET/CT–based in vivo whole-body quantification of CXCR4 receptors is viewed as a very promising diagnostic or therapeutic imaging biomarker in a variety of cancer patients [34, 35].

In this study, we present [^{68}Ga]Ga-Pentixafor PET/CT imaging results in 94 lung cancer patients and the validation of the quantitative PET parameters with simultaneous tissue characterization and quantification of CXCR4 receptors' density. To the best of our knowledge, this is the first study reporting the tracer uptake as a function of CXCR4 receptors' density identified by IHC and FACS in primary lung cancer tissue of different histologic types. We observed that all sub-types of lung cancer showed increased tracer uptake in the primary lung lesions on [^{68}Ga]Ga-Pentixafor PET, which was indicative of tumor CXCR4 overexpression. The highest CXCR4 expression was seen in SCLC, which is the most aggressive lung cancer sub-type characterized by rapid doubling time, high growth fraction, and early development of metastatic spread [36]. CXCR4 activation is also linked to metastatic behavior of cancer cells metastasizing to organs by invasive and migratory responses and adhesion to marrow stromal cells in SCLC [37, 38]. SCLC swiftly metastasizes to other organs and much more rapidly than NSCLC types. Hence, the findings of [^{68}Ga]Ga-Pentixafor SUV_{max} and MFI values highlight higher CXCR4 expression in SCLC than that in NSCLC variants which in turn validates the specificity of this in vivo CXCR4-targeting PET technique.

The IHC analysis was carried out in 11/16 patients in the group. However, none of the patients on IHC staining showed any evidence of a cytoplasmic CXCR4 tumor positivity despite that both FACS analysis and [^{68}Ga]Ga-Pentixafor findings suggested the presence of CXCR4 expression in all the patients. However, it has been reported that the digital image analysis offers an objective and quantifiable means of verifying IHC staining parameters [39]. It is pertinent to mention here that in squamous lung cancer patients, 31/54 underwent IHC staining and CXCR4 tumor positivity (mean IHC score = 5.1 ± 2.7) was seen in 29/31 patients. The inconsistency in the results of IHC with CXCR4 positivity on FACS or [^{68}Ga]Ga-Pentixafor imaging was observed in a sizeable proportion of patients, though the histopathology confirmed lung cancer in all the patients. The IHC staining accuracy is dependent upon on many technical factors, viz., tissue fixation process, dilution factor of the secondary antibody, and type and sensitivity of the antibody. We used a uniform dilution factor of 1:100 for the secondary antibodies which may not be adequate to pick up the CXCR4 cell expression in certain sub-types of patients as observed in the present study. A flow cytometry–based analysis relies on an analysis of individual cells, and it offers a higher dynamic range for signal measurement since it utilizes fluorescence rather than colorimetric measurement. However, flow cytometric measurement fails to provide information on the spatial localization of the biomarker of interest. Due to limitations associated with both methods, we have compared PET/CT SUV_{max} with the flow and IHC data.

Despite the higher CXCR4 expression (MFI) and the tracer uptake (SUV_{max}) in SCLC, we did not find a significant correlation between these two parameters which is probably due to the small number of patients ($n = 14$) in this group. In an extensive meta-analysis of 24 studies and 2037 lung cancer patients, CXCR4 was not significantly related to the prognosis factors such as age, gender, tumor size, and smoking [31]. However, these authors reported that

CXCR4 expression correlated with some prognosis factors such as N-stage (N1, N2 vs. N0), M-stage (M1 vs. M0), and tumor-stage. It has been reported that [^{68}Ga]Ga-Pentixafor PET/CT showed a higher CXCR4 receptors' density (MFI = 142.0; SUV_{max} = 13.2) in a SCLC patient than in a patient (MFI = 120.0; SUV_{max} = 8.8) with NSCLC variant [28]. It was also observed that in the SCLC patient, [^{18}F] F-FDG-PET/CT showed a SUV_{max} value of 8.0 as against the SUV_{max} value of 13.2 on [^{68}Ga]Ga-Pentixafor PET/CT. And [^{68}Ga]Ga-Pentixafor PET/CT picked up additional brain metastatic lesions in the NSCLC patient.

It is thus highlighted that [^{68}Ga]Ga-Pentixafor PET/CT demonstrating higher tracer uptake (SUV_{max}) is supported by higher receptors' density (MFI) in SCLC. The receiver operating characteristic (ROC) curve analysis of [^{68}Ga]Ga-Pentixafor SUV_{max} values provided a cutoff value of 7.2 to differentiate SCLC from NSCLC (sensitivity 87.5% and specificity 72.0%). However, no definitive trend for sensitivity and specificity with [^{18}F] F-FDG-PET/CT has been reported for this differentiation [5, 40]. In a separate study, we carried out head-to-head comparison of [^{18}F] F-FDG versus [^{68}Ga] Ga-Pentixafor PET/CT in 39 patients with different LC sub-types [41]. It was observed that though the [^{18}F] F-FDG uptake in all the LC variants was significantly higher than [^{68}Ga]Ga-Pentixafor, the sensitivity (85.7%) and specificity (78.1%) of [^{68}Ga]Ga-Pentixafor PET/CT (at SUV_{max} cutoff = 8.2) for the differentiation of SCLC versus NSCLC were significantly higher than for FDG-PET/CT (14.3%; 59.4% at SUV cutoff = 29.9).

In a recent study, Buck et al. reported that a very high [^{68}Ga]Ga-Pentixafor uptake (SUV_{max} > 12.0) was found in multiple myeloma (n = 113) followed by adrenocortical carcinoma (n = 30), mantle cell lymphoma (MCL, n = 20), adrenocortical adenoma (n = 6), and SCLC (n = 12) [23]. They concluded that these results may provide a roadmap to detect patients who may benefit from CXCR4-targeted therapies. The suitability of [^{68}Ga]Ga-Pentixafor for non-invasive high contrast imaging of CXCR4 over-expressing cancers has been demonstrated initially for hematological malignancies [42–46]. Though biopsy always remains the gold standard technique to establish the differential histopathological diagnosis of the cancer sub-type, SCLC showed high CXCR4 expression. In the present study, we performed [^{68}Ga]Ga-Pentixafor PET/CT for in vivo CXCR4 imaging and estimated the cutoff SUV_{max} values which may be useful for differentiating the lung cancer sub-types non-invasively. With the subsequent development of [^{177}Lu] Lu-Pentixather as a therapeutic companion, the first CXCR4-targeted radiotheranostic concept has been translated into the clinic [27, 47]. An encouraging therapeutic response of ^{177}Lu/^{90}Y-Pentixather for radioligand therapy (RLT) in advance stage multiple myeloma and other lymphoproliferative diseases has been reported [24–26]. The other potential therapeutic applications of this theranostic pair are being explored in prospective clinical trials.

In NSCLC and lung NEN, the mean SUV_{max} and MFI values were lower than in SCLC patients, though we did not find a significant correlation between these two parameters in SCLC. The small number of patients could be the reason in SCLC (n = 14) as in NSCLC (n = 70; squamous cell carcinoma = 54; adenocarcinoma = 16), a significant correlation was seen between SUV_{max} and CXCR4 expression. Another probable reason could be that the CXCR4 expression evaluated on the biopsied tumor tissue by the in vitro techniques is usually taken from the small portion of the lung mass. On the other hand, PET-derived SUV_{max} values represent the tracer distribution in the entire tumor volume. Therefore, NSCLC variants in addition to SCLC, with the evidence of significant CXCR4 overexpression, can also be considered for RLT using alpha- and beta-labeled CXCR4 targeting radionuclide theranostics. In a recent study, Watts et al. reported that [^{68}Ga]Ga-Pentixafor PET/CT allows non-invasive assessment of CXCR4 expression in rare lung cancers, i.e., hemangioendothelioma, sarcomatoid carcinoma, and hemangiopericytoma, and in lung metastasis cases [48]. The highest SUV_{max} of 13.0 was noted in the case of hemangioendothelioma. Therefore, the lung cancer cases other than SCLC and NSCLC which express significant quantity of CXCR4 expression also hold great potential both for imaging and treatment using ^{68}Ga-Pentixafor/^{177}Lu-Pentixather theranostic pair. The precision radiomolecular oncology using such targeted radiotheranostic approach challenging the classical statistical evidence-based medicine has been reported [49]. [^{68}Ga]Ga-Pentixafor PET/CT could be of special clinical significance in response assessment to CXCR4-based radiotherapeutics. And in a recent study, the varied physiological distribution of [^{68}Ga]Ga-Pentixafor in spleen has been reported to be of great prognostic significance [50].

[^{68}Ga]Ga-Pentixafor PET/CT scan findings indicated an increased tracer uptake (SUV_{max} = 5.2 ± 1.2) in all the 5 lung NEN patients. No significant correlation was seen between SUV_{max} and the percent stained cells (r = −0.293; p = 0.663). There is only a single study in the literature, by Werner et al., who have investigated the role of [^{68}Ga]Ga-Pentixafor in imaging GEP-NEN [51]. These authors compared the diagnostic performance of three tracers, i.e., [^{18}F] F-FDG, [^{68}Ga] Ga-DOTA-TATE, and [^{68}Ga]Ga-Pentixafor, in 12 GEP NEN patients and found concordant (positive) findings between [^{68}Ga]Ga-Pentixafor and [^{68}Ga] Ga-DOTA-TATE in 4/5 poorly differentiated NEN. However, [^{68}Ga] Ga-Pentixafor PET/CT demonstrated superiority and picked up more number (n = 66) of metastatic lesions as compared to [^{68}Ga] Ga-DOTA-TATE which detected only 12 lesions. In this regard, these authors reported that an increasing number of CXCR4 (+)/SSTR (−) metastasis were identified in patients with increasing tumor aggressiveness. The

usefulness of FDG-PET/CT in poorly dedifferentiated NEN has been described previously. These NEN variants pose a serious therapeutic challenge with the currently available [^{177}Lu] Lu-DOTA-TATE therapy and thus, [^{177}Lu] Lu-Pentixather RLT targeting CXCR4 receptors may be useful in NEN having poor SSTR expression.

Therefore, the demonstration of variable quantitative CXCR4 receptors' expression supported by the matching pattern of [^{68}Ga]Ga-Pentixafor tissue uptake in different LC sub-types provides a convincing data for using this imaging modality for radiotheranostic applications. This may potentially supplement the existing data for inclusion and expanding CXCR4-based radioligand therapies in LC beyond hematological malignancies.

Author contribution All authors contributed to the study conception and design. Ankit Watts: radiopharmaceutical synthesis, quality control testing, PET/CT imaging, image reconstruction, image quantification, IHC/FACS analysis, sample preparation, data curation, manuscript writing, and statistical analysis. Baljinder Singh: study conceptualization, manuscript editing, grant/funding to carry out the research work, supervision, project administration. Harmandeep Singh: data interpretation, PET biopsy, manuscript editing. Bhagwant R. Mittal: study designing, data interpretation, formal analysis, PET biopsy, manuscript editing, supervision. Amanjit Bal: histopathological and immunohistochemical analyses of the lung tissues, manuscript editing. Harneet Kaur: manuscript writing/editing and statistical analysis. Ninjit Dhanota: sample preparation, FACS analysis, and data interpretation. Sunil K. Arora: sample preparation, FACS analysis and data interpretation, formal analysis, supervision. Digambar Behera: study designing, patients' enrolment, clinical examination, bronchoscopy/biopsy, supervision. The first draft of the manuscript was written by AW and BS and all authors commented on previous versions of the manuscript. All authors read and approved the final manuscript.

Funding The research work was carried out using the grant by the Department of Science and Technology (DST), Government of India, under the DST-FIST program (grant SR/FST/LSI-548/2012) for setting up the infrastructure (automated chemistry module and other accessories and chemicals) required for the present work.

Data Availability The datasets generated during and/or analysed during the current study are available from the corresponding authoron reasonable request.

Declarations

Ethics approval This study was performed in line with the principles of the Declaration of Helsinki. Approval was (vide letter No. INT/IEC/2017/194 dated 23.08.2017) granted to the study as PhD project of the first author by the Institute Ethics Committee (IEC) of the Postgraduate Institute of Medical Education & Research (PGIMER), Chandigarh, India.

Competing interests The authors declare no competing interests.

References

1. AL-Jahdali H, Khan AN, Loutfi S, Al-Harbi AS. Guidelines for the role of FDG-PET/CT in lung cancer management. Journal of Infection and Public Health [Internet]. King Saud Bin Abdulaziz University for Health Sciences; 2012;5:S35–40. Available from: https://doi.org/10.1016/j.jiph.2012.09.003.
2. Baum RP, Świętaszczyk C, Prasad V. FDG-PET/CT in lung cancer: an update. Front Radiat Ther Oncol. 2010;42:15–45.
3. Kandathil A, Kay FU, Butt YM, Wachsmann JW, Subramaniam RM. Role of FDG PET/CT in the eighth edition of TNM staging of non–small cell lung cancer. Radiographics. 2018;38:2134–49.
4. Ambrosini V, Nicolini S, Caroli P, Nanni C, Massaro A, Marzola MC, et al. PET/CT imaging in different types of lung cancer: an overview. Eur J Radiol [Internet]. Elsevier Ireland Ltd; 2012;81:988–1001. Available from: https://doi.org/10.1016/j.ejrad.2011.03.020.
5. Manoharan P, Salem A, Mistry H, Gornall M, Harden S, Julyan P, et al. 18F-Fludeoxyglucose PET/CT in SCLC: analysis of the CONVERT Randomized Controlled Trial. J Thorac Oncol [Internet]. Elsevier Inc; 2019 [cited 2022 Oct 1];14:1296–305. Available from: http://www.jto.org/article/S1556086419302825/fulltext.
6. Araz M, Soydal C, Özkan E, Sen E, Nak D, Kucuk ON, et al. Prognostic value of metabolic parameters on baseline 18F-FDG PET/CT in small cell lung cancer. Q J Nucl Med Mol Imaging. 2022;66:61–6. https://doi.org/10.23736/S1824-4785.19.03169-8.
7. Xiao M, Ma X, Ma F, Li Y, Zhang G, Qiang J. Whole-tumor histogram analysis of apparent diffusion coefficient for differentiating adenosquamous carcinoma and adenocarcinoma from squamous cell carcinoma in patients with cervical cancer. Acta Radiol [Internet]. SAGE Publications; 2021;63:1415–24. Available from: https://doi.org/10.1177/02841851211035915.
8. William Strauss H, Mariani G, Volterrani D, Larson SM. Nuclear oncology: pathophysiology and clinical applications. Nuclear oncology: pathophysiology and clinical applications. 2013.
9. Park H, Sholl LM, Hatabu H, Awad MM, Nishino M. Imaging of precision therapy for lung cancer: current state of the art. Radiology. 2019;293:15–29.
10. Sarvaiya PJ, Guo D, Ulasov I, Gabikian P, Lesniak MS. Chemokines in tumor progression and metastasis. Oncotarget. 2013;4:2171–85.
11. Burger JA, Stewart DJ, Wald O, Peled A. Potential of CXCR4 antagonists for the treatment of metastatic lung cancer. Expert Rev Anticancer Ther [Internet]. Taylor & Francis; 2011;11:621–30. Available from: https://doi.org/10.1586/era.11.11.
12. Domanska UM, Kruizinga RC, Nagengast WB, Timmer-Bosscha H, Huls G, de Vries EGE, et al. A review on CXCR4/CXCL12 axis in oncology: no place to hide. Eur J Cancer [Internet]. Elsevier Ltd; 2013;49:219–30. Available from: https://doi.org/10.1016/j.ejca.2012.05.005.
13. Demmer O, Gourni E, Schumacher U, Kessler H, Wester H-JJ. PET imaging of CXCR4 receptors in cancer by a new optimized ligand. ChemMedChem [Internet]. 2011/07/20. WILEY-VCH Verlag; 2011;6:1789–91. Available from: https://pubmed.ncbi.nlm.nih.gov/21780290.
14. Demmer O, Dijkgraaf I, Schumacher U, Marinelli L, Cosconati S, Gourni E, et al. Design, synthesis, and functionalization of dimeric peptides targeting chemokine receptor CXCR4. J Med Chem [Internet]. American Chemical Society; 2011;54:7648–62. Available from: https://doi.org/10.1021/jm2009716.
15. Gourni E, Demmer O, Schottelius M, D'Alessandria C, Schulz S, Dijkgraaf I, et al. PET of CXCR4 expression by a 68Ga-labeled highly specific targeted contrast agent. J Nucl Med [Internet]. 2011;52:1803–10. Available from: http://jnm.snmjournals.org/cgi/doi/10.2967/jnumed.111.098798. Accessed 11 Apr 2016.
16. Vag T, Gerngross C, Herhaus P, Eiber M, Philipp-Abbrederis K, Graner F-P, et al. First experience with chemokine receptor CXCR4-targeted PET imaging of patients with solid cancers. Journal of Nuclear Medicine [Internet]. 2016;57:741–6. Available from: http://jnm.snmjournals.org/cgi/doi/10.2967/jnumed.115.161034. Accessed 21 Aug 2016.

17. Watts A, Singh B, Basher R, Singh H, Bal A, Kapoor R, et al. 68Ga-Pentixafor PET/CT demonstrating higher CXCR4 density in small cell lung carcinoma than in non-small cell variant. Eur J Nucl Med Mol Imaging. 2017;44:909–10.
18. Watts A, Arora D, Kumar N, Thakur S, Basher R, Radotra B, et al. 68Ga-Pentixafor PET/CT offers high contrast image for the detection of CXCR4 expression in recurrent glioma. J Nucl Med [Internet]. 2019;60:491. Available from: http://jnm.snmjournals.org/content/60/supplement_1/491.abstract.
19. Watts A, Chutani S, Arora D, Madivanane V, Thakur S, Kamboj M, et al. Automated radiosynthesis, quality control, and biodistribution of Ga-68 Pentixafor: first Indian experience. Indian J Nucl Med. Wolters Kluwer Medknow Publications; 2021;36:237–44.
20. Singh N, Aggarwal AN, Gupta D, Behera D, Jindal SK. Unchanging clinico-epidemiological profile of lung cancer in North India over three decades. Cancer Epidemiol. 2010;34:101–4.
21. Teicher BA, Fricker SP. CXCL12 (SDF-1)/CXCR4 pathway in cancer. Clin Cancer Res. 2010;16:2927–31.
22. Duda DG, Kozin SV, Kirkpatrick ND, Xu L, Fukumura D, Jain RK. CXCL12 (SDF1α)-CXCR4/CXCR7 pathway inhibition: an emerging sensitizer for anticancer therapies? Clin Cancer Res. 2011;17:2074–80.
23. Buck AK, Haug A, Dreher N, Lambertini A, Higuchi T, Lapa C, et al. Imaging of C-X-C motif chemokine receptor 4 expression in 690 patients with solid or hematologic neoplasms using 68 Ga-PentixaFor PET. J Nucl Med. Society of Nuclear Medicine; 2022;jnumed.121.263693.
24. Herrmann K, Schottelius M, Lapa C, Osl T, Poschenrieder A, Hanscheid H, et al. First-in-human experience of CXCR4-directed endoradiotherapy with 177Lu- and 90Y-labeled Pentixather in advanced-stage multiple myeloma with extensive intra- and extramedullary disease. J Nucl Med [Internet]. 2016;57:248–51. Available from: http://jnm.snmjournals.org/cgi/doi/10.2967/jnumed.115.167361. Accessed 11 Apr 2016.
25. Lapa C, Herrmann K, Schirbel A, Hänscheid H, Lückerath K, Schottelius M, et al. CXCR4-directed endoradiotherapy induces high response rates in extramedullary relapsed multiple myeloma. Theranostics [Internet]. Ivyspring International Publisher; 2017;7:1589–97. Available from: http://www.thno.org/v07p1589.htm. Accessed 8 Aug 2022.
26. Lapa C, Hänscheid H, Kircher M, Schirbel A, Wunderlich G, Werner RA, et al. Feasibility of CXCR4-directed radioligand therapy in advanced diffuse large B-cell lymphoma. J Nucl Med. Society of Nuclear Medicine Inc.; 2019;60:60–4.
27. Habringer S, Lapa C, Herhaus P, Schottelius M, Istvanffy R, Steiger K, et al. Dual targeting of acute leukemia and supporting niche by CXCR4-directed theranostics. Theranostics. Ivyspring International Publisher; 2018;8:369–83.
28. Maurer S, Herhaus P, Lippenmeyer R, Hänscheid H, Kircher M, Schirbel A, et al. Side effects of CXC-chemokine receptor 4-directed endoradiotherapy with Pentixather before hematopoietic stem cell transplantation. J Nucl Med. Society of Nuclear Medicine Inc.; 2019;60:1399–405.
29. Werner RA, Kircher S, Higuchi T, Kircher M, Schirbel A, Wester HJ, et al. CXCR4-directed imaging in solid tumors. Front Oncol. Frontiers Media S.A.; 2019;9.
30. Furusato B, Rhim JS. CXCR4 and cancer. In: Amy M. Fulton, editor. Chemokine receptors in cancer. Humana Press; 2009. p. 31–45. Available from: https://doi.org/10.1007/978-1-60327-267-4_2.
31. Shekhawat AS, Singh B, Malhotra P, Watts A, Basher R, Kaur H, et al. Imaging CXCR4 receptors expression for staging multiple myeloma by using 68Ga-Pentixafor PET/CT: comparison with 18F-FDG PET/CT. Br J Radiol. British Institute of Radiology; 2022; 1;95(1136):20211272. https://doi.org/10.1259/bjr.20211272.
32. Liang J-XX, Gao W, Liang Y, Zhou X-MM. Chemokine receptor CXCR4 expression and lung cancer prognosis: a meta-analysis. Int J Clin Exp Med [Internet]. e-Century Publishing Corporation; 2015;8:5163–74. Available from: https://pubmed.ncbi.nlm.nih.gov/26131090. Accessed 07 May 2020.
33. Spano JP, Andre F, Morat L, Sabatier L, Besse B, Combadiere C, et al. Chemokine receptor CXCR4 and early-stage non-small cell lung cancer: pattern of expression and correlation with outcome. Ann Oncol. 2004;15:613–7.
34. Buck AK, Serfling SE, Lindner T, Hänscheid H, Schirbel A, Hahner S, et al. CXCR4-targeted theranostics in oncology. Eur J Nucl Med Mol Imaging. Springer Science and Business Media LLC; 2022.
35. Buck AK, Grigoleit GU, Kraus SK, Schirbel A, Heinsch M, Dreher N, et al. C-X-C motif chemokine receptor 4-targeted radioligand therapy in patients with advanced T-cell lymphoma. J Nucl Med [Internet]. 2022;jnumed.122.264207. http://jnm.snmjournals.org/content/early/2022/06/23/jnumed.122.264207.abstract. Accessed 8 Aug 2022.
36. Oronsky B, Reid TR, Oronsky A, Carter CA. What's new in SCLC? A review. Neoplasia (United States) [Internet]. The Authors; 2017;19:842–7. Available from: https://doi.org/10.1016/j.neo.2017.07.007.
37. Burger M, Glodek A, Hartmann T, Schmitt-Gräff A, Silberstein LE, Fujii N, et al. Functional expression of CXCR4 (CD184) on small-cell lung cancer cells mediates migration, integrin activation, and adhesion to stromal cells. Oncogene. 2003;22:8093–101.
38. Bunyaviroch T, Coleman RE. PET evaluation of lung cancer. J Nucl Med. 2006;47:451–69.
39. Chlipala EA, Bendzinski CM, Dorner C, Sartan R, Copeland K, Pearce R, et al. An image analysis solution for quantification and determination of immunohistochemistry staining reproducibility. Appl Immunohistochem Mol Morphol [Internet]. 2020;28. Available from: https://journals.lww.com/appliedimmunohist/Fulltext/2020/07000/An_Image_Analysis_Solution_For_Quantification_and.3.aspx. Accessed 01 Oct 2022.
40. Burger JA, Stewart DJ. CXCR4 chemokine receptor antagonists: perspectives in SCLC. Expert Opin Investig Drugs. 2009;18:481–90.
41. Watts A, Singh B, Bal A, Kapoor R, Arora S, Mittal B, et al. 68Ga-Pentixafor PET/CT for imaging CXCR4/CXCL12 receptor-ligand axis in lung cancer - a head-to-head comparison with 18F-FDG PET/CT. J Nucl Med [Internet]. 2022;63:2266. Available from: http://jnm.snmjournals.org/content/63/supplement_2/2266.abstract.
42. Wester HJ, Keller U, Schottelius M, Beer A, Philipp-Abbrederis K, Hoffmann F, et al. Disclosing the CXCR4 expression in lymphoproliferative diseases by targeted molecular imaging. Theranostics. 2015;5:618–30.
43. Philipp-Abbrederis K, Herrmann K, Knop S, Schottelius M, Eiber M, Lückerath K, et al. In vivo molecular imaging of chemokine receptor CXCR4 expression in patients with advanced multiple myeloma. EMBO Mol Med [Internet]. BlackWell Publishing Ltd; 2015;7:477–87. Available from: http://embomolmed.embopress.org/cgi/doi/10.15252/emmm.201404698. Accessed 07 May 2020.
44. Lapa C, Schreder M, Schirbel A, Samnick S, Kortüm KM, Herrmann K, et al. [68Ga]Pentixafor-PET/CT for imaging of chemokine receptor CXCR4 expression in multiple myeloma - comparison to [18F]FDG and laboratory values. Theranostics. Ivyspring International Publisher; 2017;7:205–12.
45. Herhaus P, Habringer S, Philipp-Abbrederis K, Vag T, Gerngross C, Schottelius M, et al. Targeted positron emission tomography imaging of CXCR4 expression in patients with acute myeloid leukemia. Haematologica. Ferrata Storti Foundation; 2016;101:932–40.
46. Mayerhoefer ME, Jaeger U, Staber P, Raderer M, Wadsak W, Pfaff S, et al. [68Ga]Ga-Pentixafor PET/MRI for CXCR4 imaging of chronic lymphocytic leukemia: preliminary results. Investigative Radiology [Internet]. 2018;53. Available from: https://journals.lww.com/investigativeradiology/Fulltext/2018/07000/_68Ga_Ga_Pentixafor_PET_MRI_for_CXCR4_Imaging_of.4.aspx. Accessed 21 May 2020.

47. Schottelius M, Osl T, Poschenrieder A, Hoffmann F, Beykan S, Hänscheid H, et al. [(177)Lu]Pentixather: comprehensive preclinical characterization of a first CXCR4-directed endoradiotherapeutic agent. Theranostics [Internet]. Ivyspring International Publisher; 2017;7:2350–62. Available from: https://pubmed.ncbi.nlm.nih.gov/28744319. Accessed 21 May 2020.
48. Watts A, Singh B, Singh H, Kaur H, Bal A, Vohra M, et al. Gallium-68-Pentixafor PET/CT demonstrating in vivo CXCR4 receptors' overexpression in rare lung malignancies: correlation with the histological and histochemical findings. J Nucl Med Technol [Internet]. 2022;jnmt.122.264141. Available from: http://tech.snmjournals.org/content/early/2022/05/24/jnmt.122.264141.abstract.
49. Singh B, Kaur H, Parihar AS, Watts A, Prasad V. Precision radiomolecular oncology: challenging the classical statistical evidence-based medicine. In: Sobti RC, Dhalla NS, editors. Biomedical translational research: drug design and discovery [Internet]. Singapore: Springer Nature Singapore; 2022. p. 97–110. Available from: https://doi.org/10.1007/978-981-16-9232-1_7.
50. Serfling SE, Lapa C, Dreher N, Hartrampf PE, Rowe SP, Higuchi T, et al. Impact of tumor burden on normal organ distribution in patients imaged with CXCR4-targeted [68Ga]Ga-PentixaFor PET/CT. Mol Imaging Biol. Springer Science and Business Media Deutschland GmbH; 2022.
51. Werner RA, Weich A, Higuchi T, Schmid JS, Schirbel A, Lassmann M, et al. Imaging of chemokine receptor 4 expression in neuroendocrine tumors - a triple tracer comparative approach. Theranostics. 2017;7:1489–98.